

## Effect of Iodide Ion Substitution on the Ionic Conductivity and the Melting Point of NaBr

P. MANORAVI AND K. SHAHI\*

*Department of Physics, Indian Institute of Technology,  
Kanpur-208 016, India*

Received March 4, 1991; in revised form May 26, 1991

Ionic conductivity and the phase diagram have been studied for the NaBr-NaI system. Maximum conductivity enhancements by factors of 46, 26, and 15 with respect to pure NaBr and 2, 1.8, and 1.4 with respect to pure NaI have been obtained at  $T = 400, 500, \text{ and } 600^\circ\text{C}$ , respectively, for the composition of NaBr + 70 mole% NaI. The CBO model that predicts the composition of the mixed crystals at which the maximum conductivity occurs was found unsatisfactory for the present system. A new method for constructing the solidus curve of the phase diagram using the conductivity data alone is suggested and found satisfactory for the present NaBr-NaI system. © 1991 Academic Press, Inc.

### Introduction

There is considerable interest in solid electrolytes exhibiting relatively high ionic conductivity at near ambient temperatures. Various means such as doping the salt with aliovalent impurities, dispersion of fine insulating particles (e.g.,  $\text{Al}_2\text{O}_3$ ), and stabilizing the so-called average (disordered) structures have been used to develop new highly conducting solid electrolytes. That the mixed crystals (salts doped with homovalent ions) exhibit higher conductivity than either component member was reported quite early (1). But this was not pursued systematically as a means to increase the conductivity probably because the magnitude of enhancement reported in the early experiments (2) was not significant. However, several recent investigations (3-15) have shown that the enhancement in ionic

conductivity actually depends on the mismatch (size difference) between the host and the impurity ion, and that in a few cases (12, 13) the conductivity increases by as much as 3 orders of magnitude.

In order to explain the enhanced ionic conductivity in the mixed crystals, the idea of "lattice loosening" was briefly pointed out by Lidiard (1) and was later developed into a semiquantitative model by Shahi and Wagner (3, 4) and Johannesen and McKelvy (5, 6). According to this model, a dopant invariably has a size different (too large or too small) from the host ion, whose substitution introduces strain into the host lattice that generally results in lowering of the melting point of the mixed crystal, and hence in lowering of the formation and migration enthalpies of the defects. This leads to higher concentration and mobility of the defects and hence to high conductivity. This model has been found satisfactory for several mixed crystal systems. The report that

\* To whom correspondence should be addressed.

the defect concentration in KCl–KBr (16) is unusually large ( $\approx 1\%$ ), in sharp contradiction with the conductivity results, has since been found to be incorrect (1). The diffusion coefficient and conductivity measurements on KI–RbI (17) and KCl–KBr (18) mixed crystals fully support the view that the enhanced conductivity is essentially a defect density effect and, as a minor part, a mobility effect.

Recently, a purely thermodynamical model, called the  $CB\Omega$  model (19), was proposed which, among other things, predicts the composition of a mixed crystal corresponding to the maximum conductivity or diffusion constant ( $D$ ) (20, 21) on the basis of the compressibility and the pressure derivative of the bulk modulus of the pure end components.

This paper reports the ionic conductivity measurements on the NaBr–NaI system and examines the validity of the lattice loosening and the  $CB\Omega$  models. Since a good correlation exists between the increase in  $\sigma$  and decrease in melting point of the mixed crystals, it is shown that the conductivity data can be effectively used to predict a part of the phase diagram, i.e., the solidus curve.

## Experimental

High purity NaBr and NaI (Aldrich Chemicals) were dried in vacuum at temperature  $>200^\circ\text{C}$  for about 20 hr and subsequently stored inside a dry box. The gas purification system (Mecaplex, Model 2-667/2) keeps the moisture and oxygen contents, inside the dry box, less than a few parts per million. To prepare the mixed crystals, appropriate amounts of NaBr and NaI were weighed, thoroughly mixed, and then melted in a quartz tube followed by cooling to room temperature and grinding into a fine powder. The cylindrical pellets (diameter  $\approx 1$  cm, thickness 2–3 mm) prepared from this powder were annealed at suitably high tem-

peratures for 20 hr after loading them in the sample holder. Platinum paint was used as electrodes. The entire operations starting from material preparation up to conductivity studies were done in a dry nitrogen atmosphere inside the dry box. The impedance measurements were carried out using a HP 4192A low-frequency impedance analyzer. The DTA (LINSEIS Model L62) was used for the phase diagram study with a typical heating/cooling rate of  $5^\circ\text{C}/\text{min}$ .

## Results and Discussion

### 1. Conductivity vs Composition

The complex impedance analysis method was used to obtain the dc conductivity data. Figure 1 shows the conductivity vs composition isotherms at three different temperatures. Since our primary aim was to investigate the conductivity enhancement due to homovalent dopants, only the intrinsic conductivity and the extrapolated intrinsic conductivity at lower temperatures were considered while drawing the conductivity isotherms. It is observed in Fig. 1 that as the concentration of NaI increases, the ionic conductivity of the mixed crystal also increases, goes through a maximum at a composition of  $\sim 70$  mole% NaI, and starts decreasing subsequently. It is also evident that the enhancement in conductivity is more prominent at lower temperatures. Maximum enhancements by factors of 46, 26, and 15 with respect to pure NaBr and 2, 1.8, and 1.4 with respect to pure NaI are observed at  $T = 400^\circ\text{C}$ ,  $500^\circ\text{C}$ , and  $600^\circ\text{C}$ , respectively for the composition of 70 mole% NaI.

Recently a theoretical model, called the  $CB\Omega$  model, which predicts the composition ( $x_m$ ) corresponding to the maximum conductivity and the diffusion coefficient in alkali halide mixed crystals, was proposed (19–21). According to this model,  $x_m$  is given by

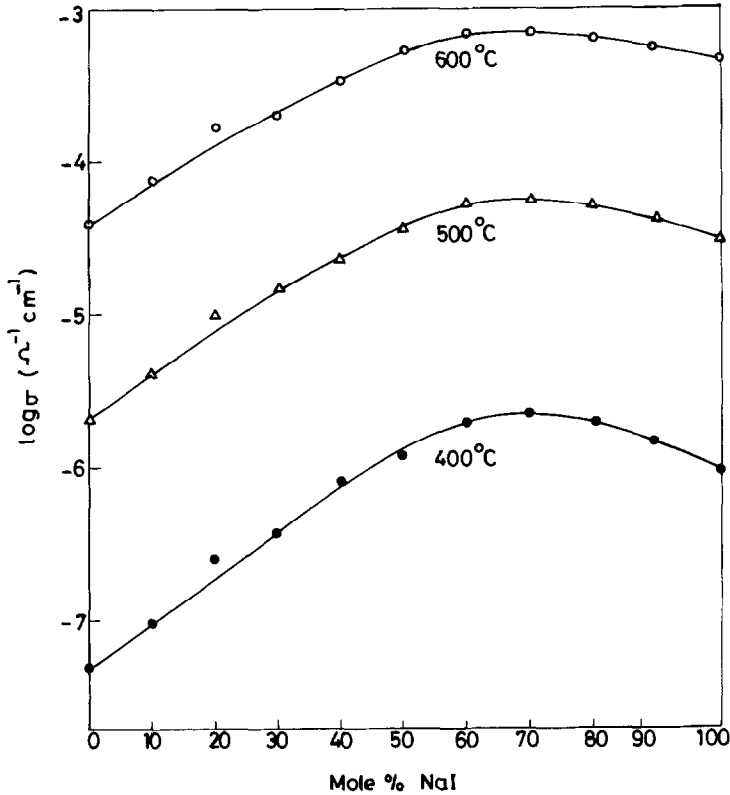


FIG. 1. Logarithm of conductivity vs composition (mole%) of the mixed crystal  $\text{NaBr}_{1-x}\text{I}_x$  at 400, 500, and 600°C. The curve corresponding to 400°C is based on conductivity data obtained by extrapolating the linear  $\log \sigma$  vs  $1/T$  plot (intrinsic region) to 400°C.

$$x_m = \frac{(k^d/k^l) - 2}{\lambda(k^d/k^l)}, \quad (1)$$

where  $k^d$  and  $k^l$  are the compressibilities of the defect volume and the pure component, respectively. The ratio  $k^d/k^l$  is given by

$$\frac{k^d}{k^l} = 1 + \frac{4(n+3)}{9(dB^1/dP - 1)}, \quad (2)$$

where  $n$  and  $dB^1/dP$  are respectively the Born's exponent and the pressure derivative of the isothermal bulk modulus of the pure crystals. The  $\lambda$  in Eq. (1) is defined as

$$\lambda = \frac{V_2}{V_1} - 1, \quad (3)$$

where  $V_1$  and  $V_2$  are the molar volumes of the two end members.

By considering NaBr as the pure component and NaI as the dopant and substituting the corresponding values of  $n$ ,  $dB/dP$ , and  $\lambda$  (22, 23) into Eqs. (2) and (3), we get

$$k^d/k^l = 2.222 \quad \text{and} \quad \lambda = 0.269.$$

The substitution of these values into Eq. (1) gives

$$x_m = 0.37.$$

Thus, the NaBr–NaI mixed crystal system should exhibit a maximum in the conductivity at ~37 mole% NaI.

However, if we consider NaI as the pure component and NaBr as the second component (dopant), we get

$$x_m = 0.40,$$

i.e., the conductivity maximum for NaBr–NaI should be at 40 mole% NaBr (or 60 mole% NaI). This model therefore predicts the existence of a pair of maxima or a maximum in the range  $37 < (\text{mole}\%) \text{ NaI} < 60$ . The fact that the actual maximum occurs at 70 mole% NaI shows the limitation of this theory, even though the conditions of the CBΩ model (21), viz, that

$$k^d/k^l \geq 2 \quad \text{and} \quad 1 - \frac{2}{(k^d/k^l)} \leq \lambda,$$

are well satisfied by the present NaBr–NaI system. Thus it would appear that the above model, which was found satisfactory for several systems (11, 20, 21), needs modifications to widen its generality. At this stage we would, however, wish to point out that the success of the model depends critically on the experimental values of input parameters such as  $k^d$ ,  $k^l$ , etc. An uncertainty of  $\pm 2\%$  in the values of  $dB/dP$  (23, 24) which does not seem unrealistic, leads to an error of  $\mp 8\%$  in the values of  $x_m$ . In addition, there is some ambiguity about the value of Born's exponent  $n$ . Thus, the validity of the CBΩ model cannot be questioned simply on the basis of the discrepancy pointed out above.

## 2. Conductivity vs Temperature

Figures 2 and 3 show the  $\log \sigma$  vs  $1/T$  plots for solid solutions  $\text{NaBr}_{1-x}\text{I}_x$  in the range  $0 \leq x \leq 0.7$  and  $0.7 \leq x \leq 1$ , respectively. The conductivity–temperature behavior can be described by an Arrhenius equation,

$$\sigma = A \exp(-E_a/kT). \quad (4)$$

The  $\log \sigma$  vs  $1/T$  plots consist of two linear regions, viz., the intrinsic and the extrinsic

regions, separated by a knee point ( $T_N$ ). The preexponential factor, the activation energy (both intrinsic and extrinsic), and the  $T_N$  for various compositions are given in Table I.

The variations of intrinsic activation energy and  $T_N$  as a function of composition are shown in Figs. 4 and 5, respectively. While the conductivity increases due to the substitution of homovalent dopants, both the intrinsic activation energy ( $E_a$ ) and the knee temperature ( $T_N$ ) decrease. As expected, while  $E_a$  vs composition and  $T_N$  vs composition plots exhibit a minimum at around the same composition (70 mole% NaI) at which the  $\sigma$  vs composition plot exhibits a maximum. Since the activation energy is a measure of the energy of formation and migration of the defects, these results are qualitatively in agreement with the lattice loosening model (2–5, 11) which predicts that the substitution of wrong size ions introduces strain into the host lattice, weakens the bonding between the ions, and decreases the energy of formation and migration of the defects.

## 3. Phase Diagram

The liquidus and the solidus curves of the phase diagram of NaBr–NaI system, as inferred from the DTA studies, are shown in Fig. 6. The literature values (25) corresponding to the liquidus curve are also shown for comparison. There is good agreement between the two results as far as the nature of the liquidus curve is concerned. However, the previous values (25) of the melting points of pure as well as mixed crystals are consistently higher (by  $\sim 10^\circ\text{C}$ ) than the present values. Both the liquidus and the solidus curves exhibit a minimum at  $\sim 70$  mole% NaI; the lowest melting point observed is  $\sim 630^\circ\text{C}$ , which is about 107 and  $21^\circ\text{C}$  lower than those of pure NaBr and NaI, respectively. The liquidus and the solidus temperatures of all compositions studied are listed in Table I. The fact that the minimum in the melting point and the maxi-

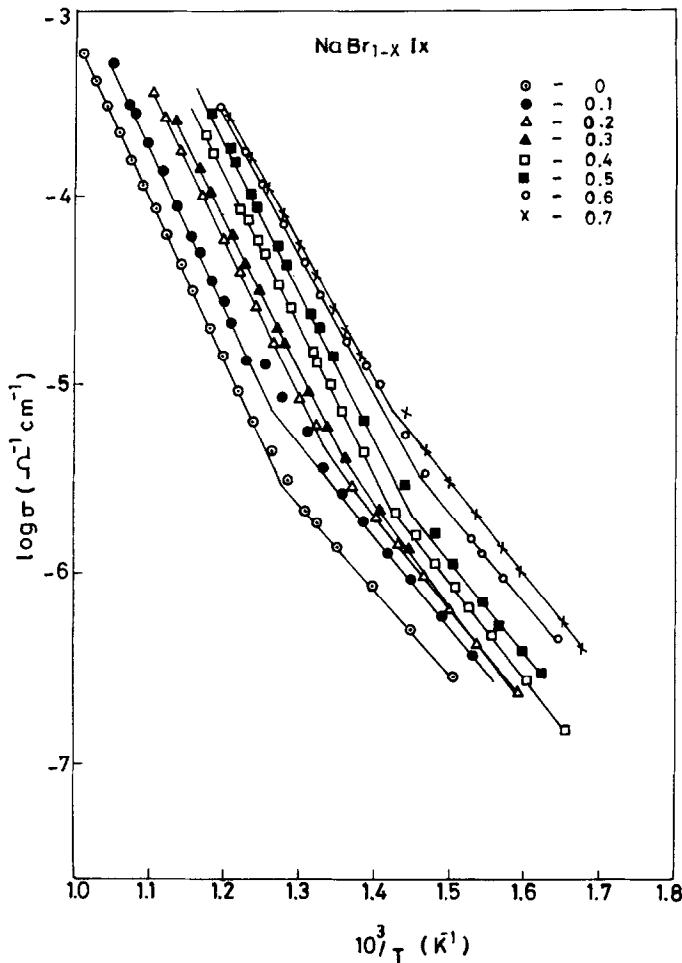


FIG. 2. Logarithm of conductivity vs inverse temperature for NaBr<sub>1-x</sub>I<sub>x</sub> (0 ≤ x ≤ 0.7) solid solutions.

mum in the conductivity occur at the same composition (~70 mole% NaI) suggests that the lattice loosening model is indeed relevant.

Figure 7 shows the temperature ( $T_{\sigma}$ ) at which a mixed crystal attains a certain (fixed) value of conductivity as a function of composition.  $T_{\sigma 1}$  and  $T_{\sigma 2}$  correspond to two different fixed values of conductivity,  $5 \times 10^{-5}$  and  $10^{-5}$  ohm<sup>-1</sup> cm<sup>-1</sup>. These curves are essentially constructed from the data shown in Figs. 2 and 3. The solidus curve ( $T_{ms}$ ) of the phase diagram (Fig. 6) is also

shown in Fig. 7. It is evident that the nature of the  $T_{\sigma}$  and  $T_m$  curves is surprisingly similar. Similar results for KBr–NaBr (11) and KBr–NaI (12) have already been reported. In fact the resemblance between  $T_m$  vs composition and  $T_{\sigma}$  vs composition curves is so close that it would appear entirely possible to predict the phase diagram (solidus curve) from the measured conductivity vs composition behavior.

Both NaBr and NaI exhibit Schottky type defects, and hence, the basic defect mechanism in the mixed NaBr–NaI crystals is ex-

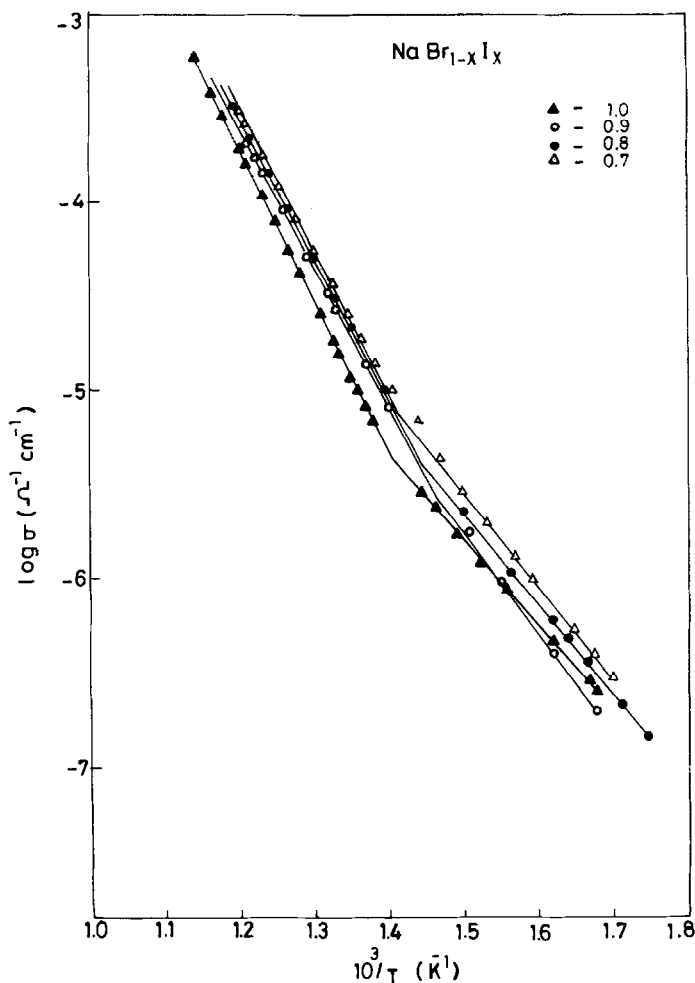


FIG. 3. Logarithm of conductivity vs inverse temperature for  $\text{NaBr}_{1-x}\text{I}_x$  ( $0.7 \leq x \leq 1$ ) solid solutions.

pected to be the same as that in the parent phases. Further, the cation vacancies in pure as well as in the mixed crystals are found to be more mobile than that of the anion vacancies (17, 18). Thus the ratio of the ionic conductivity of the mixed crystal ( $\sigma_x$ ) to that of pure crystal ( $\sigma_0$ ) at temperature ( $T$ ) can be approximated by (2-5, 11, 12)

$$\frac{\sigma_x}{\sigma_0} \approx \exp\left(-\frac{1/2\Delta H + \Delta h}{kT}\right), \quad (5)$$

where  $\Delta H = H_x - H_0$

$$\Delta h = h_x - h_0$$

and  $H_x$  and  $H_0$  are the enthalpies of formation of Schottky defects in the mixed and pure crystal, respectively and  $h_x$  and  $h_0$  are the respective enthalpies of migration of defects. The variation in the preexponential factors of the Arrhenius equation (Eq. 4) is ignored because the change in the entropy of formation and migration of defects between pure and mixed crystals will not be very different (2-5).

The formation enthalpy,  $H$ , and the mi-

TABLE I  
MELTING (LIQUIDUS  $T_L$  AND SOLIDUS  $T_S$ ) TEMPERATURES AND THE IONIC TRANSPORT PARAMETERS  
OF THE NaBr-NaI MIXED CRYSTAL SYSTEM

Mole% of NaI in NaBr	$E_a$ intrinsic (eV)	$E_a$ extrinsic (eV)	$A$ intrinsic ( $\Omega^{-1} \text{ cm}^{-1}$ )	Knee temperature ( $^{\circ}\text{C}$ )	$T_L$ ( $^{\circ}\text{C}$ )	$T_S$ ( $^{\circ}\text{C}$ )
0	1.71	0.88	$2.53 \times 10^5$	531	737	737
10	1.68	1.11	$3.51 \times 10^5$	490	717	705
20	1.64	1.02	$5.32 \times 10^5$	472	796	675
30	1.60	1.12	$3.01 \times 10^5$	466	677	660
40	1.57	1.00	$3.87 \times 10^5$	434	661	646
50	1.55	1.04	$4.34 \times 10^5$	415	646	641
60	1.48	1.12	$2.43 \times 10^5$	410	638	633
70	1.44	0.97	$1.38 \times 10^5$	426	630	629
80	1.48	1.05	$2.05 \times 10^5$	413	638	634
90	1.52	0.95	$4.36 \times 10^5$	424	644	639
100	1.57	0.88	$5.57 \times 10^5$	439	651	651

gration enthalpy,  $h$ , are empirically related to the melting point ( $T_m$ ) of the salt (26–30),

$$H = \alpha T_m \quad (\text{eV}) \quad (6)$$

and

$$h = \beta T_m - C \quad (\text{eV}), \quad (7)$$

where  $\alpha$  ( $= 2.14 \times 10^{-3} \text{ eV K}^{-1}$ ),  $\beta$  ( $= 0.84 \times 10^{-3} \text{ eV K}^{-1}$ ), and  $C$  ( $= 0.2 \text{ eV}$ ) are constants (26, 27). It has been demonstrated

earlier (11, 12) as well as in the present case (Fig. 7) that it is the solidus (rather than the liquidus) temperature that satisfies better the above correlations (Eqs. (6) and (7)) and hence should be identified as the melting point ( $T_m$ ) of the mixed crystal. The change in the melting (solidus) temperature of the mixed crystal is then given by

$$\Delta T_{ms} = T_{ms} - T_{mo}, \quad (8)$$

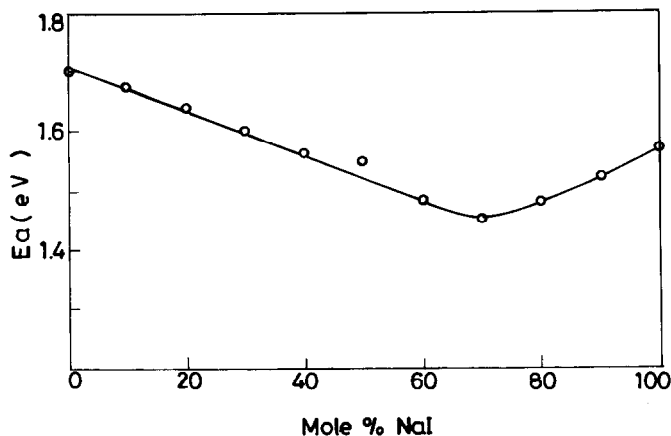


FIG. 4. Activation energy ( $E_a$ , intrinsic region) vs composition (mole% NaI in NaBr).

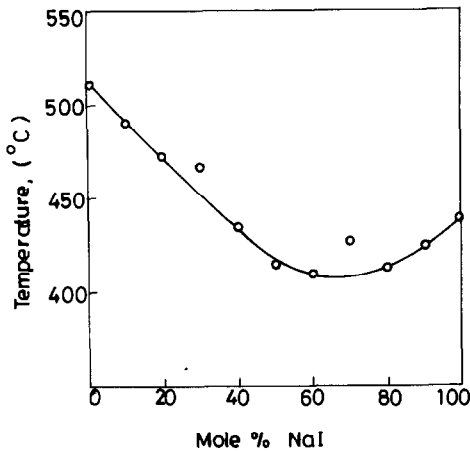


FIG. 5. Knee temperature ( $T_N$ ) vs composition (mole% NaI in NaBr).

where  $T_{ms}$  is the melting (solidus) temperature of the mixed crystal and  $T_{mo}$ , the melting temperature of the pure salt ( $T_{ms} = T_{mo}$  for the pure salt).

Substituting Eqs. (6), (7), and (8) into Eq. (5) yields

$$\frac{\sigma_x}{\sigma_0} \approx \exp\left(-\frac{(1/2\alpha + \beta)\Delta T_{ms}}{kT}\right)$$

or

$$\Delta T_{ms} \approx -4.5 \times 10^{-2} T \ln(\sigma_x/\sigma_0). \quad (9)$$

The above equation predicts the change in the melting point of a mixed crystal if the relative conductivity ( $\sigma_x/\sigma_0$ ) is known at some temperature ( $T$ ). Since  $\sigma_x$  is generally greater than  $\sigma_0$  or  $\sigma_x/\sigma_0 \geq 1$ , Eq. (9) correctly suggests that the  $\Delta T_{ms}$  is negative; i.e., the melting point of the mixed crystal generally decreases as a result of doping. Figure 8 compares the melting (solidus) curve obtained from DTA with that obtained from Eq. (9). It should be emphasized that the calculated curve shown in Fig. 8 is based on three sets of data points obtained corresponding to conductivity isotherms at three

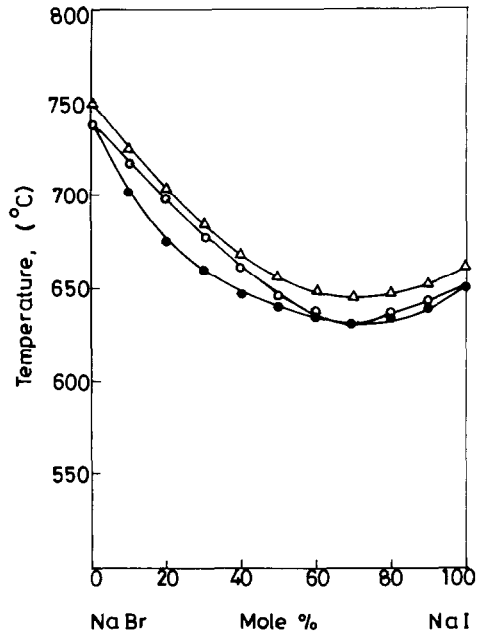


FIG. 6. Phase diagram of NaBr-NaI system: (○) liquidus ( $T_L$ ); and (●) solidus ( $T_S$ ) temperature vs composition (mole% NaI in NaBr). (△) Melting points (liquidus) according to Ref. (25).

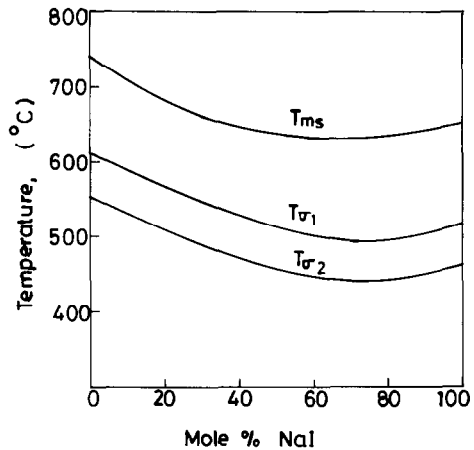


FIG. 7. Temperature at which a mixed crystal attains a fixed conductivity, i.e.,  $T_\sigma$ , as a function of composition (mole% NaI in NaBr).  $T_{\sigma_1}$  and  $T_{\sigma_2}$  refer to curves corresponding to two different fixed conductivities,  $\sigma_1 = 5 \times 10^{-5}$  and  $\sigma_2 = 10^{-5} \Omega^{-1} \text{cm}^{-1}$ . The  $T_{ms}$  curve is the melting (solidus) curve of the phase diagram (Fig. 6).



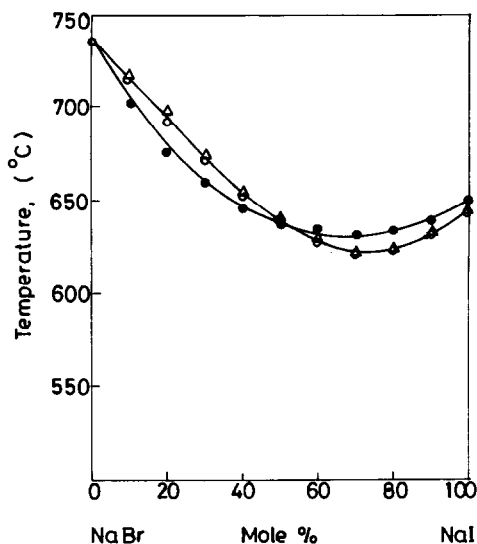


FIG. 8. Solidus curve of the phase diagram: (●) experimental, (○, △) calculated from conductivity studies; Eq. (9).

different temperatures (Fig. 1).<sup>1</sup> Both curves exhibit minima at around the same composition (~70 mole% NaI). The largest discrepancy between the two results (Fig. 8) is about 10°C which is small (~9%) compared to the maximum change in the melting point (of ~110°C for 70 mole% NaI) or negligible (~1.1%) compared to the melting point (~903°K) of the mixed crystal itself. This discrepancy may be partly or wholly attributed to:

(i) The errors in the experimental determination of melting points from DTA. This itself could easily account for a 5–10°C error in the measured  $T_m$  values.

(ii) The approximation that the preexponential factor remains unaffected by doping, leading to a simplified version of the relative

<sup>1</sup> In case the conductivity falls in the extrinsic region for the temperature considered, only the extrapolated intrinsic values of conductivity to that temperature in the linear  $\log \sigma$  vs  $1/T$  plots should be taken for calculations.

conductivity expression (Eq. 5) and hence that of  $\Delta T_m$  (Eq. 9).

(iii) The assumption that the anionic contribution to total conductivity is negligible. In view of these observations, a discrepancy of 10°C between the observed and the calculated  $T_m$  values is not at all a serious matter.

The solid solution/two-phase boundary (demixing curve) could not be studied using DTA because of the small thermic effects associated with that process. The conductivity studies can also be used to obtain the demixing curve separating the two regions by using the fact that as soon as the phase separation (in the cooling cycle) sets in, the conductivity deviates from the standard Arrhenius behavior (11, 30, 31). Since no such behavior is observed in our  $\log \sigma$  vs  $1/T$  plots, which extend down to 350°C, we can safely assume that NaBr and NaI form a complete solid solution at least above 350°C.

## Conclusions

There is appreciable enhancement in the conductivity due to the substitution of homovalent ions; viz.,  $I^-$  in NaBr and  $Br^-$  in NaI. The maximum enhancement in  $\sigma$  (by a factor of 46 at 400°C) is observed for the  $NaBr_{0.3}I_{0.7}$  solid solution, which also has a minimum melting point (630°C) and the lowest activation energy (1.44 eV). These results are completely consistent with the lattice loosening model.

Even though the conductivity results on NaBr–NaI do not directly support the CBΩ model, it has been argued that its relevance cannot be ruled out.

The lattice loosening model allows the calculation of the solidus curve of the phase diagram from the conductivity data on mixed crystals. This can be used as an additional tool to determine part of the binary phase diagrams of ionic solids.

## References

1. A. B. LIDIARD, "Handbuch der Physik" (S. Flügge, Ed.), Vol. 20, p. 246 (1957).

2. H. SHULZE, Ph.D thesis, University of Göttingen (1952) as cited in Ref (1).
3. K. SHAHI AND J. B. WAGNER, *J. Phys. Chem. Solids*, **44**(2), 89 (1983).
4. K. SHAHI AND J. B. WAGNER, *Solid State Ionics* **12**, 511 (1984).
5. O. JOHANNESSEN AND M. MCKELVY, *Solid State Ionics* **17**, 251 (1985).
6. O. JOHANNESSEN AND M. MCKELVY, *J. Phys. Chem. Solids* **47**(3), 265 (1986).
7. O. JOHANNESSEN "Proceedings of the 6th International Conference on Solid State Ionics, Garmisch-Partenkirchen, FRG, Sept. 6-11" p. 1310 (1987).
8. K. SHAHI AND J. B. WAGNER, *J. Phys. Chem. Solids* **43**(8), 713 (1982).
9. S. IHARA, Y. WARITA, AND K. SUZUKI, *Phys. Status Solidi A* **86**, 729 (1984).
10. T. BHIMA SANKARAM AND K. G. BANSIGIR, *Cryst. Lattice Defects* **7**, 209 (1978).
11. P. MANORAVI AND K. SHAHI, *J. Phys. Chem. Solids*, **52**, 527 (1991).
12. P. MANORAVI AND K. SHAHI, *Solid State Ionics* **45**, 83 (1991).
13. V. N. EROFEEV AND E. HARTMANN, *Solid State Ionics* **28-30**, 241, (1988).
14. P. MERCIER, M. TACHZ, J. P. MALGUANI, AND G. ROBERT, *Solid State Ionics* **15**, 109 (1985).
15. S. GUPTA, S. PATNAIK, S. CHAKLANOBIS, AND K. SHAHI, *Solid State Ionics* **31**, 5 (1988).
16. W. E. WALLACE AND R. A. FLINN, *Nature* **172**, 681 (1953).
17. L. BONPUNT, N. B. CHANH, G. COMBERTON, Y. HAGET, AND F. BENIERE, *Radiat. Eff.* **75**, 33 (1983).
18. F. BENIERE AND V. HARIBABU, *Cryst. Latt. Def. Amorphous Mater.* **15**, 263 (1987).
19. P. VAROTSOS, W. LUDWIG, AND K. ALEXOPOULOS, *Phys. Rev. B* **18**, 2683 (1978).
20. P. VAROTSOS, *J. Phys. Chem. Solids* **42**, 405 (1981).
21. P. A. VAROTSOS AND K. D. ALEXOPOULOS, "Thermodynamics of Point Defects and Their Relations with Bulk Properties." North-Holland, Amsterdam (1986).
22. C. S. SMITH AND L. S. CAIN, *J. Phys. Chem. Solids* **36**, 205 (1978).
23. R. W. ROBERTS AND C. S. SMITH, *J. Phys. Chem. Solids* **31**, 619 (1970).
24. D. S. PURI AND M. P. VERMA, *Phys. Rev. B* **15**, 2337 (1977).
25. International Critical Tables, Vol. IV, pp. 40-72. McGraw-Hill, New York (1928).
26. L. W. BARR AND LIDIARD, "Physical Chemistry. An Advanced Treatise," Vol. 10, p. 151. Academic Press, New York (1970).
27. L. W. BARR AND D. K. DAWSON, *Proc. Brit. Ceramic Soc.*, **19**, 151 (1971).
28. W. BOLLMANN, *Phys. Status Solidi A* **61**, 395 (1980).
29. N. F. UVAROV, E. F. HAIRETDINOV, AND W. BOLLMANN, *Cryst. Res. Technol.* **24**(4), 413 (1989).
30. W. BOLLMANN, N. F. UVAROV, AND E. F. HAIRETDINOV, *Cryst. Res. Technol.* **24**(4), 421 (1989).
31. A. SCHIRALDI, E. PEZZATI, AND G. CHIODELLI, *Z. Phys. Chem. Neue Folge.* **110**, 1 (1978).
32. A. SCHIRALDI AND E. PEZZATI, *Z. Phys. Chem. Neue Folge.* **113**, 179 (1978).